

## Spiropyrans and spirooxazines

### 2.\* Synthesis, structures, and photochromic properties of 6'-cyano-substituted spironaphthooxazines

N. A. Voloshin,<sup>a</sup> A. V. Metelitsa,<sup>a\*</sup> J. C. Micheau,<sup>b</sup> E. N. Voloshina,<sup>c</sup> S. O. Besugliy,<sup>a</sup> N. E. Shelepin,<sup>a</sup>  
V. I. Minkin,<sup>a</sup> V. V. Tkachev,<sup>d</sup> B. B. Safoklov,<sup>d</sup> and S. M. Aldoshin<sup>d</sup>

<sup>a</sup>Institute of Physical and Organic Chemistry, Rostov State University,  
194/2 prosp. Stachki, 344090 Rostov-on-Don, Russian Federation.

Fax: +7 (863 2) 43 4667. E-mail: photo@ipoc.rsu.ru

<sup>b</sup>Paul Sabatier University, UMR CNRS 5623, IMRCP,  
118 route de Narbonne, F-31062 Toulouse, France. \*\*

E-mail: micheau@chimie.ups-tlse.fr

<sup>c</sup>Department of Chemistry, Rostov State University,  
7 ul. Zorge, 344090 Rostov-on-Don, Russian Federation.

Fax: +7 (863 2) 22 3957

<sup>d</sup>Institute of Problems of Chemical Physics, Russian Academy of Sciences,  
142432 Chernogolovka, Moscow Region, Russian Federation.

Fax: +7 (096) 515 3588. E-mail: sma@icp.ac.ru

A series of 6'-cyano-substituted spiro[indoline-2,3'-naphtho[2,1-*b*]oxazines] containing substituents with carbon chains of different lengths in the indoline fragment were synthesized. The structure of one of these spironaphthooxazines was established by X-ray diffraction analysis. The influence of substituents on the photochromic properties of the resulting compounds in solutions and polymeric films was studied.

**Key words:** spironaphthooxazines, synthesis, X-ray diffraction analysis, photochromic properties, structure—properties correlation.

Diverse possible fields of application of organic photochromic compounds impose vast demands on their characteristics.<sup>2a–6</sup> In this connection, the directed synthesis, which allows one to reveal general characteristic features responsible for the relationship between the molecular structures of photochromic compounds and their spectroscopic and kinetic properties, assumes great importance. Among photochromes, spirocyclic compounds are distinguished by the fact that their molecular structures can be rather easily modified. The introduction of electron-releasing and electron-withdrawing substituents into spiropyrans and spirooxazines leads to the electron density redistribution both in the spiro units and the conjugated bond systems of the starting and photoinduced forms of these compounds, as well as to a change in the characteristics of photochromic transformations.<sup>2a,3,7</sup> Bulky substituents, for example, long-chain linear or branched alkyl groups, can also substantially influence

photochromic transformations, particularly, in viscous media.<sup>3,5–9</sup>

Since spirooxazines (SPO) are much more resistant to photodegradation<sup>2b,10</sup> compared to spiropyrans, the former compounds hold more promise for the practical use in materials with variable optical density. Earlier, it has been demonstrated<sup>11,12</sup> that the introduction of the CN group at position 6' of spironaphthooxazine leads to a substantial change in the photochromic characteristics. The aim of the present study was to synthesize a series of new 6'-cyano-substituted spironaphthooxazines and investigate their spectroscopic and kinetic properties.

## Results and Discussion

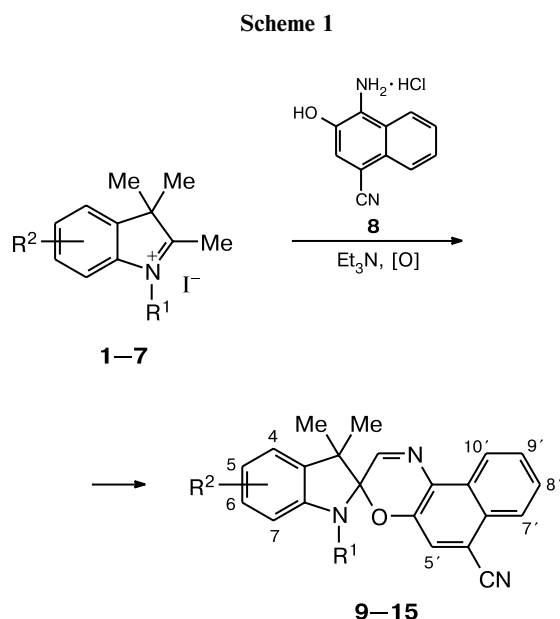
**Synthesis and structures of 6'-cyano-substituted spironaphthooxazines.** The most commonly used procedure for the preparation of SPO is based on the synthesis from aromatic *o*-hydroxynitroso compounds and alkylidene derivatives of aromatic heterocycles, which are generally generated *in situ* by the reactions of bases with the corresponding quaternary salts.<sup>2b,3,7</sup>

\* For Part 1, see Ref. 1.

\*\* Universite Paul Sabatier, UMR CNRS 5623, IMRCP, 118 route de Narbonne, F-31062 Toulouse, France.

6'-Cyano-substituted spirooxazines were prepared according to a procedure, which we have developed recently for the synthesis of SPO, by condensation of aminonaphthols with alkylidene derivatives of aromatic heterocycles in the presence of an oxidizing agent. Presumably, this reaction proceeds through the formation of ketene generated upon oxidation of methylene base.<sup>13</sup> We chose this method because it is easier to synthesize cyano-substituted aminonaphthol than to produce the corresponding nitrosonaphthol required for the preparation of 6'-cyano-substituted spirooxazines according to the conventional procedure.

We synthesized (Scheme 1) 6'-cyano-substituted spiroindolinaphthooxazines **9–15** for the first time. These compounds were prepared by the reactions of 3*H*-indolium iodides **1–7** with 1-amino-4-cyano-2-naphthol hydrochloride (**8**) in the presence of Et<sub>3</sub>N and DMSO as an oxidizing agent.



**1, 9:** R<sup>1</sup> = Pr, R<sup>2</sup> = 5-OMe; **2, 10:** R<sup>1</sup> = Bu<sup>i</sup>, R<sup>2</sup> = 5-OMe;  
**3, 11:** R<sup>1</sup> = Me, R<sup>2</sup> = 5-OPr; **4, 12:** R<sup>1</sup> = Me, R<sup>2</sup> = 5-OC<sub>9</sub>H<sub>19</sub>;  
**5, 13:** R<sup>1</sup> = Me, R<sup>2</sup> = 5-OC<sub>16</sub>H<sub>33</sub>;  
**6, 14:** R<sup>1</sup> = Me, R<sup>2</sup> = 5-Me, 4(6)-Me;  
**7, 15:** R<sup>1</sup> = Me, R<sup>2</sup> = 4(6)-OMe

The starting 3*H*-indolium iodides **1–7**, 1-amino-4-cyano-2-naphthol hydrochloride (**8**), and 1,3,3-trimethylspiro[indoline-2,3'-[3*H*]naphtho[2,1-*b*][1,4]oxazine] (**16**) were synthesized according to procedures described earlier.<sup>1,3a,14–16</sup> Iodides **6** and **7** were prepared as a mixture of 4,5- and 5,6-dimethyl derivatives and a mixture of 5- and 6-methoxy derivatives, respectively, because the corresponding indolenines were generated as mixtures of isomeric products, which were used without separation.

Compound **14** was prepared as a mixture of isomeric 4,5- (**14a**) and 5,6-dimethyl-substituted (**14b**) derivatives.

Compound **15** was produced as a mixture of isomeric 4- (**15a**) and 6-methoxy (**15b**) derivatives.

The structures of compounds **9–15** were established by <sup>1</sup>H NMR spectroscopy. The structure of compound **10** was additionally confirmed by X-ray diffraction analysis.

The <sup>1</sup>H NMR spectra of compounds **14** and **15** represent the sums of the spectra of isomers **14a,b** and **15a,b**, respectively. The isomer contents, which were determined from the integral intensities of the readily identifiable signals for the protons, were 59 and 41% for **14a,b** and 64 and 36% for **15a,b**.

According to the results of X-ray diffraction analysis, spirooxazine **10** crystallized in the monoclinic system.

**Table 1.** Principal crystallographic parameters and characteristics of X-ray diffraction study of compound **10**

Parameter	<b>10</b>
Formula	C <sub>27</sub> H <sub>27</sub> N <sub>3</sub> O <sub>2</sub>
Molecular weight	425.52
Crystal system	Monoclinic
Space group	<i>P</i> 2(1)/ <i>n</i>
<i>a</i> /Å	12.076(2)
<i>b</i> /Å	11.479(2)
<i>c</i> /Å	17.394(3)
β/deg	108.60(3)
<i>V</i> /Å <sup>3</sup>	2285.2(7)
<i>Z</i>	4
<i>d</i> <sub>calc</sub> /g cm <sup>-3</sup>	1.237
<i>F</i> (000)	904
<i>R</i>	0.042
<i>R</i> <sub>w</sub>	0.0896
GOF( <i>F</i> <sup>2</sup> )	0.877

**Table 2.** Bond lengths (*d*) in molecule **10**

Bond	<i>d</i> /Å	Bond	<i>d</i> /Å
O(1)—C(4)	1.367(2)	C(7)—C(8)	1.417(3)
O(1)—C(1)	1.469(2)	C(7)—C(12)	1.417(3)
O(2)—C(27)	1.192(7)	C(8)—C(9)	1.416(3)
O(2)—C(21)	1.386(3)	C(9)—C(10)	1.362(4)
N(1)—C(2)	1.271(3)	C(10)—C(11)	1.401(4)
N(1)—C(3)	1.411(3)	C(11)—C(12)	1.361(4)
N(2)—C(18)	1.408(2)	C(14)—C(15)	1.527(3)
N(2)—C(1)	1.433(3)	C(15)—C(16)	1.514(4)
N(2)—C(14)	1.457(3)	C(15)—C(17)	1.520(4)
N(3)—C(13)	1.149(3)	C(18)—C(19)	1.379(3)
C(1)—C(2)	1.513(3)	C(18)—C(23)	1.391(3)
C(1)—C(24)	1.565(3)	C(19)—C(20)	1.403(4)
C(3)—C(4)	1.379(3)	C(20)—C(21)	1.370(4)
C(3)—C(8)	1.421(3)	C(21)—C(22)	1.380(4)
C(4)—C(5)	1.398(3)	C(22)—C(23)	1.377(3)
C(5)—C(6)	1.375(3)	C(23)—C(24)	1.512(3)
C(6)—C(7)	1.428(3)	C(24)—C(26)	1.522(3)
C(6)—C(13)	1.437(3)	C(24)—C(25)	1.541(3)

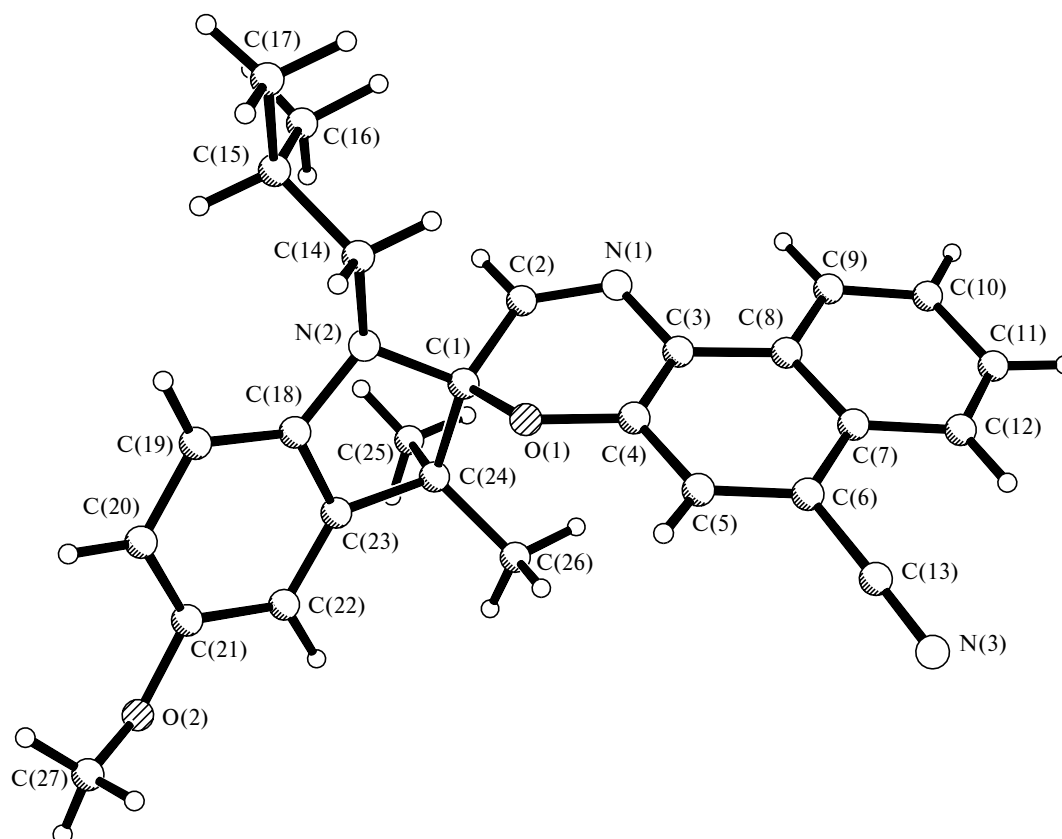


**Fig. 1.** Overall view of molecule **10**.

The crystallographic data and principal characteristics of the refinement are given in Table 1. The overall view of the molecule is shown in Fig. 1. Selected bond lengths and bond angles are listed in Tables 2 and 3, respectively.

Compound **10** is structurally similar to spirooxazines and spiropyrans studied earlier.<sup>4a,17</sup> The indoline fragment in **10** is virtually orthogonal to the naphthooxazine fragment. The indoline ring is nonplanar and adopts an

**Table 3.** Bond angles ( $\omega$ ) in molecule **10**

Angle	$\omega/\text{deg}$	Angle	$\omega/\text{deg}$	Angle	$\omega/\text{deg}$
C(4)—O(1)—C(1)	116.9(1)	C(6)—C(5)—C(4)	119.1(2)	C(19)—C(18)—C(23)	120.6(2)
C(27)—O(2)—C(21)	127.0(4)	C(5)—C(6)—C(7)	122.0(2)	C(19)—C(18)—N(2)	129.5(2)
C(2)—N(1)—C(3)	116.6(2)	C(5)—C(6)—C(13)	118.4(2)	C(23)—C(18)—N(2)	109.9(2)
C(18)—N(2)—C(1)	107.7(2)	C(7)—C(6)—C(13)	119.5(2)	C(18)—C(19)—C(20)	117.8(3)
C(18)—N(2)—C(14)	120.8(2)	C(8)—C(7)—C(12)	119.3(2)	C(21)—C(20)—C(19)	121.3(2)
C(1)—N(2)—C(14)	119.9(2)	C(8)—C(7)—C(6)	117.9(2)	C(20)—C(21)—C(22)	120.5(2)
N(2)—C(1)—O(1)	107.3(1)	C(12)—C(7)—C(6)	122.7(2)	C(20)—C(21)—O(2)	123.6(3)
N(2)—C(1)—C(2)	111.0(2)	C(7)—C(8)—C(9)	118.9(2)	C(22)—C(21)—O(2)	115.9(3)
O(1)—C(1)—C(2)	108.9(2)	C(7)—C(8)—C(3)	119.3(2)	C(21)—C(22)—C(23)	119.0(3)
N(2)—C(1)—C(24)	103.9(2)	C(9)—C(8)—C(3)	121.8(2)	C(22)—C(23)—C(18)	120.8(2)
O(1)—C(1)—C(24)	109.6(2)	C(10)—C(9)—C(8)	120.3(3)	C(22)—C(23)—C(24)	130.3(2)
C(2)—C(1)—C(24)	115.6(2)	C(9)—C(10)—C(11)	120.5(3)	C(18)—C(23)—C(24)	108.9(2)
N(1)—C(2)—C(1)	126.5(2)	C(12)—C(11)—C(10)	121.1(3)	C(23)—C(24)—C(26)	114.0(2)
C(4)—C(3)—N(1)	120.6(2)	C(11)—C(12)—C(7)	119.8(3)	C(23)—C(24)—C(25)	108.7(2)
C(4)—C(3)—C(8)	120.4(2)	N(3)—C(13)—C(6)	176.7(3)	C(26)—C(24)—C(25)	109.3(2)
N(1)—C(3)—C(8)	118.9(2)	N(2)—C(14)—C(15)	114.4(2)	C(23)—C(24)—C(1)	99.9(2)
O(1)—C(4)—C(3)	121.3(2)	C(16)—C(15)—C(17)	110.9(3)	C(26)—C(24)—C(1)	114.2(2)
O(1)—C(4)—C(5)	117.5(2)	C(16)—C(15)—C(14)	112.1(2)	C(25)—C(24)—C(1)	110.3(2)
C(3)—C(4)—C(5)	121.2(2)	C(17)—C(15)—C(14)	108.5(2)		

**Table 4.** Spectroscopic and kinetic characteristics of spirooxazines **9–16**

Com- pound	Solution in toluene				Solution in MeOH			
	$\lambda_{\max}^A$ /nm	$\varepsilon_{\max}^A$ /L mol <sup>-1</sup> cm <sup>-1</sup>	$\lambda_{\max}^B$ /nm	$k_{B \rightarrow A} \cdot 10^2/s^{-1}$ (293 K)	$\lambda_{\max}^A$ /nm	$\varepsilon_{\max}^A$ /L mol <sup>-1</sup> cm <sup>-1</sup>	$\lambda_{\max}^B$ /nm	$k_{B \rightarrow A} \cdot 10^2/s^{-1}$ (293 K)
<b>9</b>	318, 331, 373	8764, 7937, 7273	662	0.841	316, 329, 372	8910, 8218, 7358	655	0.024
<b>10</b>	318, 332, 373	8535, 8189, 7650	662	0.781	316, 329, 372	9298, 8698, 8000	657	0.021
<b>11</b>	318, 332, 372	8849, 8047, 7634	662	1.007	316, 328, 370	9290, 8530, 7910	650	0.028
<b>12</b>	318, 331, 372	8876, 8080, 7663	662	1.033	316, 328, 371	9320, 8530, 7840	651	0.027
<b>13</b>	318, 331, 372	8472, 7594, 7353	662	1.029	316, 328, 370	8475, 7768, 7106	651	0.027
<b>14</b>	303, 318, 331, 372	5722, 5901, 7348, 7790	651	1.013	302, 316, 330, 370	6230, 6584, 7912, 8053	644	0.043
<b>15</b>	332, 370	7452, 7471	645	4.347	329, 369	8105, 7871	642	0.219
<b>16</b>	319, 348	7638, 5412	596	19.14	318, 347	6802, 4714	613	27.18

Note.  $\lambda_{\max}^A$  and  $\lambda_{\max}^B$  are the long-wavelength absorption maxima of forms **A** and **B**, respectively (see Scheme 2);  $\varepsilon_{\max}^A$  is the molar extinction coefficient;  $k_{B \rightarrow A}$  is the rate constant of the thermal reverse reaction.

envelope conformation. The folding angle along the N(2)...C(24) line (30.4°) falls within the range of the values observed in the compounds of this type studied earlier (26.7–39.9°). The naphthooxazine fragment is also nonplanar, as characterized by the dihedral angles between the planes passing through the O(1), C(2), C(1) and O(1), C(2), N(1) atoms (18.3°) and between the planes passing through the O(1), C(2), N(1) and O(1), N(1), C(3), C(4) atoms (13.3°).

In compound **10**, the N(2) atom deviates from the C(18)C(1)C(14) plane by 0.11 Å and the sum of the angles at the N atom is 347.57°. The N(2)—C(1) bond length is 1.433(3) Å, which is in analogy with the compounds of this type studied earlier.<sup>4a,17</sup> The orientations of the bonds at the N(2) atom indicate that the lone electron pair (LEP) of the N atom is in the *trans* arrangement with respect to the C(1)—O(1) bond. The LEP-N(2)—C(1)—O(1) torsion angle is 1.3°. The structure of the spiro unit indicates that the antibonding  $\sigma^*$  orbital of the C(1)—O(1) bond is virtually parallel to the lone electron pair of the N(2) atom. This orientation is favorable for the orbital interaction between the n-lone electron pair of the N(2) atom and the antibonding  $\sigma^*$  orbital of the C(1)—O(1) bond. This interaction should lead to strengthening and shortening of the C(1)—N(2) bond, as well as to weakening and elongation of the C(1)—O(1) bond. Actually, the bond lengths at the C<sub>spiro</sub> atom confirm the presence of this interaction. Thus, the C<sub>spiro</sub>—O bond (1.469(2) Å) is elongated, whereas the N(2)—C<sub>spiro</sub> bond (1.433(3) Å) is shortened compared to the standard values for such bonds (C<sub>spiro</sub>—O = 1.471–1.497 Å, N(2)—C<sub>spiro</sub> = 1.434–1.453 Å).<sup>18</sup> The efficiency of the n- $\sigma^*$  interaction depends also on the electronic state of the heteroatoms at the spiro unit. The presence of a strong electron-withdrawing substituent at the C(6) atom of the naphthalene fragment should influence the electronic state of the N(1) and O(1) atoms thus

increasing conjugation of the N(1)=C(2)  $\pi$ -bond and the  $\pi$ -lone electron pair of the O(1) atom with the  $\pi$ -system of the naphthalene fragment. In molecule **10**, the N(1)—C(3) and O(1)—C(4) bond lengths (1.411(3) and 1.367 Å, respectively) are typical of compounds belonging to a series of indoline-containing spiropyranes.<sup>4a</sup> Correspondingly, the C(1)—O(1) bond (1.469(2) Å) in SPO **10**, which is cleaved upon photoexcitation, tends to be elongated compared to the standard bond of this type.<sup>18</sup>

On the whole, the distribution of the bond lengths in the naphthooxazine fragment of molecule **10** can be related to the effect of the CN substituent, which exhibits the negative inductive (*-I*) and negative mesomeric (*-M*) effects (see Table 2).

**Spectroscopic and photochemical studies of spirooxazines.** Studies by electronic absorption spectroscopy and kinetic investigations of the spirooxazines synthesized were carried out in solutions and polymeric matrices. The results of these studies are summarized in Tables 4–6.

**Table 5.** Spectroscopic and kinetic characteristics of spirooxazines **9–15** in poly(methyl methacrylate)

Com- pound	$\lambda_{\max}^{\text{A}}$	$\lambda_{\max}^{\text{B}}$	$\tau_{1/2}^{\text{B/s}}$ (293 K)	$\eta$
	nm			
<b>9</b>	375	671	750	0.39
<b>10</b>	375	671	217	0.39
<b>11</b>	374	667	523	0.35
<b>12</b>	374	669	712	0.36
<b>13</b>	374	667	875	0.38
<b>14</b>	373	660	332	0.49
<b>15</b>	372	650	325	0.41

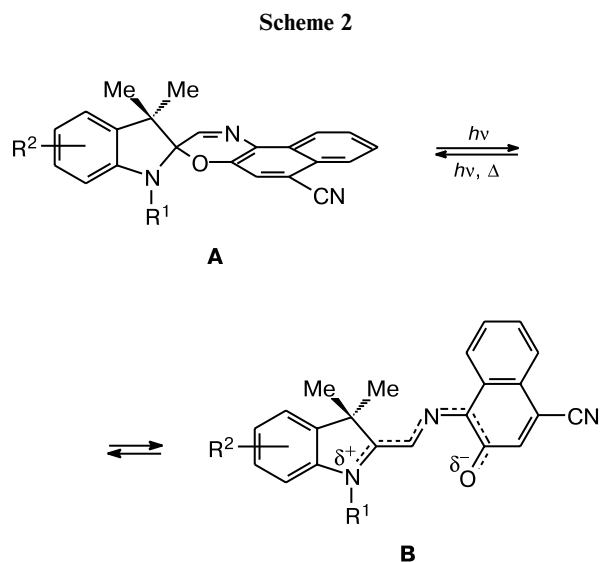
Note. For conventional notations, see Table 4;  $\tau_{1/2}^B$  is the parameter describing the kinetics of thermal decoloration,  $\eta$  is the relative photocolability.

**Table 6.** Results of modeling of the kinetics of the thermal reverse reactions of spirooxazines **9–15** in poly(methyl methacrylate) by Eq. (1) and the Kohlrausch–Williams–Watts (KWW) function

Compound	Model												KWW		
	$i = 2$					$i = 3$									
	$k_1$	$k_2$	$D_1$	$D_2$	$R^2$	$k_1$	$k_2$	$k_3$	$D_1$	$D_2$	$D_3$	$R^2$	$k'/s^{-1}$	$\alpha$	$R^2$
	$s^{-1}$					$s^{-1}$									
<b>9</b>	0.0128	0.0015	0.4011	0.4522	0.9992	0.0323	0.0061	0.0011	0.1773	0.3629	0.3559	0.99997	0.0525	0.39	0.9983
<b>10</b>	0.0132	0.0015	0.3664	0.4121	0.99914	0.0333	0.0062	0.0011	0.1643	0.3270	0.3270	0.99997	0.0549	0.38	0.9986
<b>11</b>	0.0128	0.0015	0.2644	0.3004	0.99918	0.0323	0.0061	0.0011	0.1417	0.2473	0.2398	0.99997	0.0534	0.38	0.9983
<b>12</b>	0.0128	0.0014	0.1679	0.2103	0.99913	0.0333	0.0060	0.0010	0.0754	0.1516	0.1729	0.99997	0.0473	0.38	0.9984
<b>13</b>	0.0121	0.0014	0.1842	0.2091	0.99927	0.0294	0.0058	0.0010	0.0824	0.1634	0.1694	0.99998	0.0575	0.35	0.9975
<b>14</b>	0.0161	0.0017	0.3236	0.3050	0.99866	0.0385	0.0071	0.0011	0.1592	0.2690	0.2330	0.99995	0.0835	0.31	0.9986
<b>15</b>	0.0196	0.0020	0.1796	0.1416	0.99826	0.0435	0.0080	0.0013	0.0960	0.1399	0.1000	0.99994	0.1179	0.27	0.9976

Note.  $k_i$  and  $D_i$  are the first-order rate constant and the amplitude factor for the  $i$ -th expansion term, respectively;  $R^2$  is the determination coefficient;  $k'$  is the first-order rate constant;  $\alpha$  is the parameter specifying the range of deviations from the first-order reaction kinetics.

In the electronic absorption spectra of solutions of SPO **9–15**, the long-wavelength absorption maxima of cyclic isomers **A** (Scheme 2) are in the range of 369–372 nm and are virtually independent of the steric (the length of the alkyl substituent) and electronic (the presence and positions of electron-releasing groups) properties of the substituents in the indoline moiety of the molecule (see Table 4).



By contrast, the presence of the strong electron-withdrawing substituent, *viz.*, the CN group, in the naphthooxazine moiety of SPO **9–15** leads to a substantial bathochromic shift of the absorption maximum of form **A** in the spectra of these compounds compared to unsubstituted SPO **16** (see Table 4). This fact is consistent with the assumption of both the additivity of the elec-

tronic absorption spectra of the noncoplanar fragments of SPO and localization of the electron transfer, which is responsible for the longest-wavelength absorption band, on the naphthooxazine moiety.<sup>19</sup>

Upon irradiation of solutions of compounds **9–15** in the absorption bands of cyclic forms **A**, the evolution of the photoinduced processes (cleavage of the C–O bond and subsequent *cis–trans* isomerizations) was completed with the formation of colored metastable product **B**<sup>7</sup> typical of SPO (see Scheme 2 and Fig. 2). Substantial bathochromic shifts of the absorption maxima of acyclic isomers **B** in the series of compounds **9–15** compared to unsubstituted SPO **16** are associated primarily with the presence of the electron-withdrawing CN group in the naphthooxazine fragment (for example, *cf.*  $\lambda_{\max}^B$  for

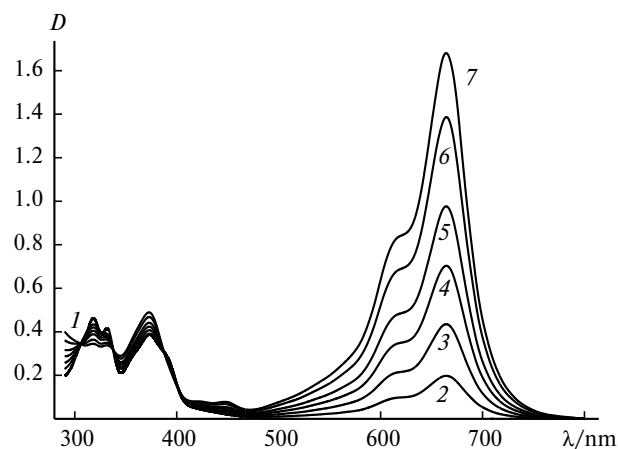


**Fig. 2.** Electronic absorption spectra of spirooxazine **10** in toluene ( $C = 5.1 \cdot 10^{-5}$  mol L<sup>-1</sup>,  $T = 293$  K) before (**I**) and after irradiation with light ( $\lambda = 365$  nm) for 3 (**2**), 7 (**3**), 14 (**4**), 21 (**5**), 40 (**6**), and 90 s (**7**).

SPO **14** and **16** in Table 4) and, to a somewhat lesser, extent with the presence of the electron-releasing OAlk groups at position 5 (the *para* position with respect to the N atom of the indoline ring) of the indoline moiety of SPO (*cf.*  $\lambda_{\max}^B$  for SPO **14** and **9–13** in Table 4) in contrast to the MeO group at position 4(6) (the *meta* position with respect to the N atom of the indoline ring) of SPO **15**.

Analysis of the dependence of the spectroscopic characteristics of photomerocyanines **B** on empirical Brooker's parameters of the solvents,  $\chi_R$  and  $\chi_B$ , allows one to estimate their polar properties.<sup>20</sup> For 6'-cyano-substituted SPO **9–15**, it was found that the frequencies of the absorption maxima of acyclic isomers **B** correlate with the parameters  $\chi_B$  and do not correlated with the parameters  $\chi_R$ , which is indicative of negative solvatochromism (Fig. 3). The observed effect is evidence for charge delocalization in the ground state of photomerocyanines resulting in stabilization of the bipolar structure. For unsubstituted SPO **16**, there is, on the contrary, a correlation between the frequencies of the absorption maxima of

color form **B** and the parameters  $\chi_R$ , whereas the correlation with the parameters  $\chi_B$  is not observed (see Fig. 3, *a*, *b*). In this case, positive solvatochromism is a consequence of weak polarity of the ground state of the acyclic isomer, *i.e.*, the predominantly quinoid structure of photomerocyanine **B**.

The most substantial effect on the photochromic properties of SPO upon the introduction of the CN group into the naphthooxazine fragment is associated with sharp deceleration of the thermal reverse reaction (*cf.* the constants  $k_{B \rightarrow A}$  for SPO **16** and **9–15** in Table 4). After termination of irradiation, merocyanines underwent cyclization into the starting SPO. Figure 4 demonstrates the linear dependence of the logarithm of the relative change in the absorbance of solutions of SPO at the absorption maximum of the photoinduced isomers in the course of thermal decoloration. As can be seen from this figure, the kinetics of the latter process obeys a monoexponential law and depends both on the structure of SPO **9–15** and the nature of the solvent (see Table 4). In the series of 6'-cyano-substituted SPO **9–15**, the bulky alkyl substituents at the N atom substantially influence the rate constant of the thermal reverse reaction ( $k_{B \rightarrow A}$ ) resulting in its decrease (see Table 4). However, the length of the alkyl chain of the OAlk group at position 5 in the series of compounds **11–13** has virtually no effect on the kinetics of the relaxation process.

Compounds **14** and **15** were prepared as mixtures of two isomers, which differ in the position of the substituent (4 or 6) in the indoline fragment and, strictly speaking, cannot be correctly analyzed. Nevertheless, particular conclusions can be made based on studies of thermal decoloration of solutions of these samples. For example, the monoexponential approximation of the kinetics of the **B**  $\rightarrow$  **A** recyclization shown in Fig. 4 is characterized by a

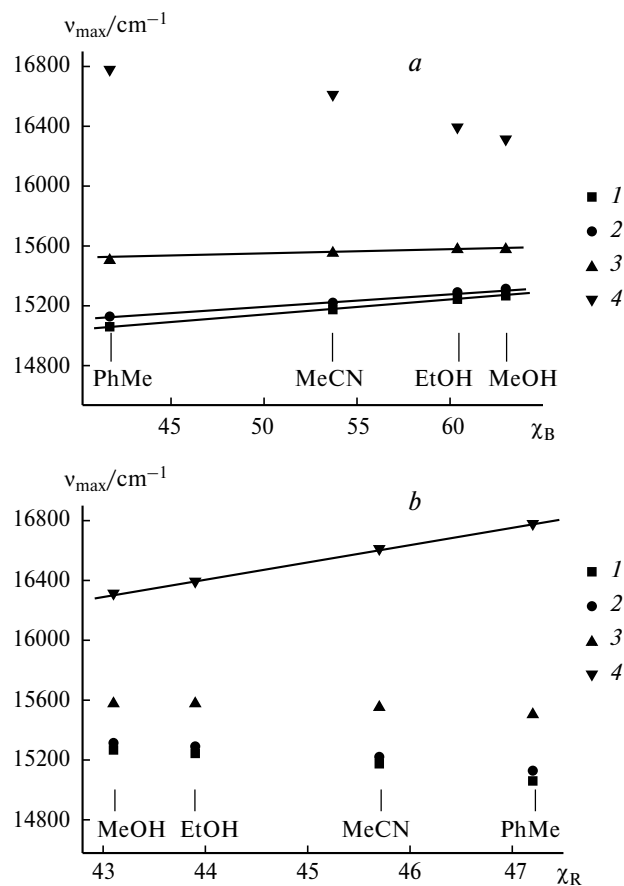


Fig. 3. Frequency of the long-wavelength absorption maximum ( $v_{\max}$ ) of the merocyanine form of spirooxazines **9** (**1**), **13** (**2**), **15** (**3**), and **16** (**4**) vs. Brooker's parameters of the solvents  $\chi_B$  (*a*) and  $\chi_R$  (*b*).

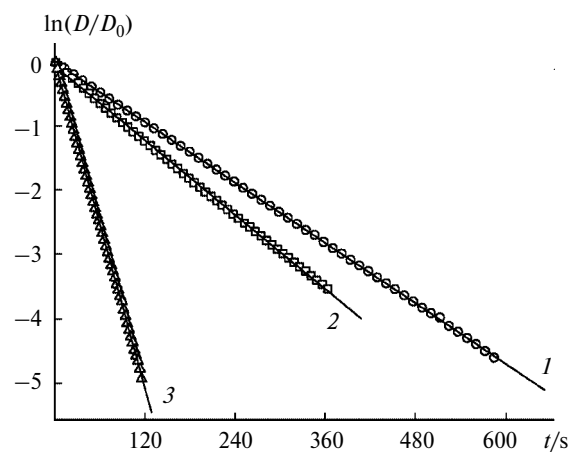


Fig. 4. Changes in the logarithm of the relative change in the absorbance ( $D/D_0$ ) of solutions of spirooxazines **10** (**1**), **14** (**2**), and **15** (**3**) in toluene ( $T = 293$  K) at the absorption maximum of the photoinduced isomers in the course of thermal decoloration.

high determination coefficient ( $R^2 = 0.9997\text{--}0.9999$ ) both in the case of isomeric mixtures of **14** and **15** as well as of individual compounds **9**–**13** (data for SPO **10** are given as an example). This fact implies that the properties (at least those associated with thermal recyclization) of 4-substituted spirooxazines are very similar to those of 6-substituted spirooxazines. Therefore, positions 4 and 6 of the indoline fragment are equally accessible for replacing groups. This conclusion can be considered as indirect evidence for the bipolar structure of merocyanine form **B** of compounds **9**–**15**, whereas the positive charge is localized on the N atom of the indoline moiety of SPO. In this case, the mesomeric effect of substitution at position 4 is equal to that at position 6 because both these positions are *meta* positions with respect to the N atom. By contrast, the replacement at position 5 (the *para* position) leads to a sharp change in the kinetic characteristics of thermal decoloration (for example, cf.  $k_{B \rightarrow A}$  for SPO **11** and **15** in Table 4).

Bipolarity of the acyclic isomers of 6'-cyano-substituted SPO **9**–**15** is manifested in the fact that the rate constant of the  $B \rightarrow A$  thermal reaction decreases as the polarity of the solvent increases, whereas the rate constant of the thermal transformation of the quinoid isomer of unsubstituted SPO **16** increases with increasing polarity of the solvent (Fig. 5).<sup>7</sup> The kinetics of thermal reactions of the bipolar structures is to a larger extent influenced by specific interactions with protic solvents (alcohols) through intermolecular hydrogen bonding. For example, the monotonic dependence of the rate constant of thermal decoloration on the dielectric permeability of the solvent observed for unsubstituted SPO **16** is violated for compounds **9**–**15** in the series of solvents, including alcohols (see Fig. 5).

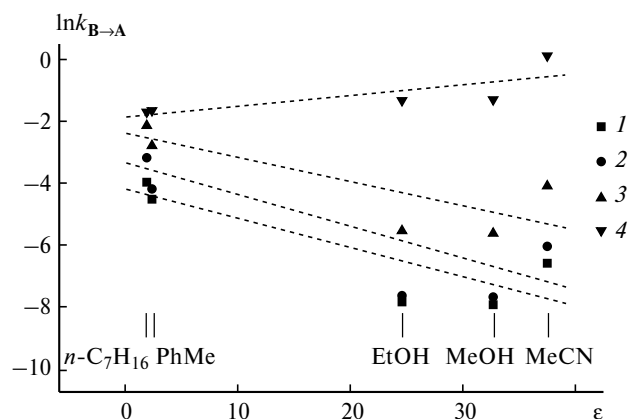


Fig. 5. Logarithm of the rate constant of thermal decoloration ( $\ln k_{B \rightarrow A}$ ) of solutions of spirooxazines **10** (1), **13** (2), **15** (3), and **16** (4) vs. the polar properties of the solvent described by the dielectric permeability ( $\epsilon$ ) at  $T = 293$  K (tendencies for a change, viz., an increase in  $\ln k_{B \rightarrow A}$  with increasing  $\epsilon$  for spirooxazine **16** and a decrease in  $\ln k_{B \rightarrow A}$  for compounds **10**, **13**, and **15** are shown by dashed lines).

The experimental facts, which are indicative of the bipolar structure of the merocyanine form of compounds **9**–**15**, unlike the quinoid structure of the colored form of unsubstituted SPO **16**, are to a large extent determined by the electron-withdrawing properties of the CN group. The presence of the strong electron-withdrawing CN group in the naphthooxazine fragment leads to delocalization of the negative charge on the O atom thus stabilizing the bipolar structure of the merocyanine form. In compounds **9**–**13** and **15**, the additional effect acting in the same direction is associated with the introduction of the electron-releasing OAlk groups into the indoline fragment of SPO. These groups facilitate delocalization of the positive charge on the N atom. The effect of the OAlk groups is more pronounced in the case of the *para*-substitution (position 5, compounds **9**–**13**) rather than in the case of the *meta*-substitution (positions 4 and 6, compound **15**) with respect to the N atom of the indoline fragment.

The efficiency of the photoinduced reactions giving rise to merocyanine forms **B** of compounds **9**–**15** in poly(methyl methacrylate) (PMMA) is 0.35–0.49 as expressed in terms of the relative photocolability ( $\eta$ ) (see Table 5). The values of the parameter  $\eta$  characterize 6'-cyano-substituted spirooxazines as efficient photochromes ( $\eta = 1$  for 1',3',3'-trimethyl-6-nitrospiro[2H-1-benzopyran-2,2'-indoline] (6-nitroBIPS), which is one of the best photochromes of the class of spirocyclic compounds). The structural differences between compounds **9**–**15** associated with the size of the alkyl groups in the indoline moiety have no substantial effect on their colorability. The largest value of  $\eta$  is achieved for compound **14** deprived of electron-releasing alkoxy groups in the indoline fragment.

The dependence of the spectroscopic characteristics of isomeric forms **A** and **B** of 6'-cyano-substituted spirooxazines in PMMA (see Table 5) on the structure is analogous to the above-considered dependence for solutions (see Table 4).

The kinetics of dark decoloration of compounds **9**–**15** in PMMA, unlike the kinetics in solutions, does not obey a monoexponential law. The approximate estimation based on the parameter  $\tau_{1/2}^B$  gave the dependence of the thermal processes on the molecular structures of spirooxazines qualitatively similar to that observed for solutions (see Table 5). Quantitative analysis of the observed kinetic curves can be carried out using the multiexponential function described by Eq. (1)<sup>21</sup>

$$D(\lambda) = \sum D_{0,i}(\lambda) \exp(-k_i t), \quad (1)$$

where  $D(\lambda)$  is the absorbance, which changes with time due to the thermal reverse reaction, in the absorption band of the photoinduced form at the wavelength  $\lambda$ ;  $D_{0,i}(\lambda)$  and  $k_i$  are the amplitude factor and the first-order rate constant for the  $i$ -th expansion term, respectively. Even

for the biexponential approximation ( $i = 2$ ), the determination coefficient is 0.999 (see Table 6). The consideration of three exponents ( $i = 3$ ) made it possible to achieve  $R^2 = 0.9999$ . It should be noted that within the framework of the above-mentioned approximations ( $i = 2, 3$ ), the pre-exponential factors  $D_{0,i}$  are of the same order of magnitude (see Table 6). Evidently, the consideration of a larger number of terms in Eq. (1) will allow one to achieve better agreement with experimental data. In this approach, the results are, however, difficult to interpret in the context of the structure dependence of each of the processes, which were found by mathematical simulation and which follow the monoexponential law (for example, due to the existence of different isomeric forms of colored product **B**). In the general case, the existence and, correspondingly, manifestation of different isomers of the open form must not be ruled out. Hence, one would expect that upon the expansion according to Eq. (1), the predominant contribution characterized by the pre-exponential factors  $D_{0,i}$  will belong to the number of terms corresponding to the number of isomeric forms. However, this presumption was not confirmed (see Table 6).

An alternative description of deviations from the first-order reaction kinetics is based on a nonuniform distribution of the free volume in a polymer resulting in the deviation of the characteristics of the molecules introduced into the polymer. This description seems to be more preferable. The relaxation functions describing different phenomena in disordered solid media can be approximated by the Kohlrausch—Williams—Watts (KWW) function<sup>22</sup>

$$K(t) = k' t^{\alpha-1}, \quad (2)$$

$$0 < \alpha \leq 1.$$

In Eq. (2),  $k'$  is the first-order rate constant and  $t$  is the time. If  $\alpha = 1$ ,  $K(t) = k'$ , *i.e.*, the parameter  $\alpha$  characterizes the range of deviations from the first-order reaction kinetics. Based on the KWW function, the following equation for the time-dependent rate constant  $k_t$  was derived:<sup>23</sup>

$$\log k_t = (\alpha - 1) \log t + \log k'. \quad (3)$$

The experimental constants  $k_t$  can be determined from the equation  $k_t = -d \ln C(t)/dt = -d \ln D(t)/dt$ , where  $C(t)$  is the concentration function of time. In the region of individual absorption, the absorbance function of time  $D(t)$  can be used instead of the concentration function.

The dependences of  $\log k_t$  on  $\log t$  thus obtained are well described by linear functions (Fig. 6). The parameters  $\alpha$  and  $k'$  found according to Eq. (3) are given in Table 6. Spirooxazine **15** appeared to be most sensitive to the nonuniform distribution of the free volume. The parameter  $\alpha$  for this compound is indicative of the largest degree of deviation from the first-order kinetics. The con-

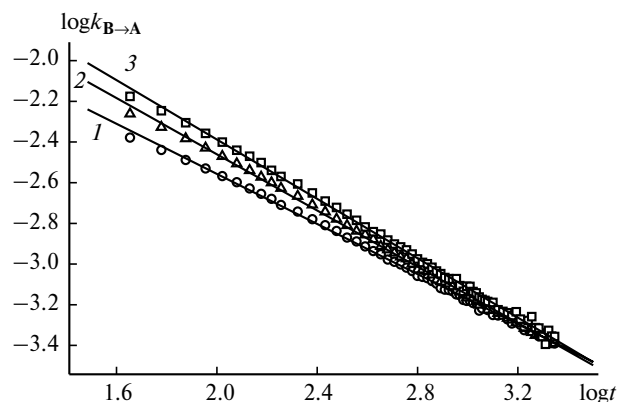


Fig. 6. Logarithm of the rate constant of thermal decoloration ( $\log k_{B \rightarrow A}$ ) of spirooxazines **12** (1), **14** (2), and **15** (3) in poly(methyl methacrylate) vs.  $\log t$  at  $T = 293$  K.

stants  $k'$  can serve as a characteristic of thermal decoloration of SPO in PMMA. The constants  $k'$  correlate better with the rate constants of the reverse reactions of spirooxazines in MeOH, which may be a consequence of the polar properties of PMMA.

To summarize, we synthesized a series of new 6'-cyano-substituted spirooxazines containing alkyl and alkoxy substituents with carbon chains of different lengths in the indoline fragment. The molecular structure of 6'-cyano-1-isobutyl-5-methoxy-3,3-dimethylspiro[indoline-2,3'-[3*H*]naphtho[2,1-*b*][1,4]oxazine] was established by X-ray diffraction analysis. The structure of the latter compound is similar to those of spirooxazines and spiropyran studied earlier. It was demonstrated that the spectroscopic and kinetic properties of the spirooxazines under study, *viz.*, the bathochromic shift of the long-wavelength absorption maximum of the photoproduct and its high thermal stability, are determined by the bipolar structure of the merocyanine form stabilized by the electron-withdrawing CN group in the naphthooxazine fragment. Deviations of the relaxation processes observed for these spirooxazines in PMMA from the first-order reaction kinetics are associated with the nonuniform distribution of the free volume and are adequately described by the Kohlrausch—Williams—Watts function.

## Experimental

The  $^1\text{H}$  NMR spectra were recorded on a Varian Unity-300 spectrometer (300 MHz) in  $\text{CDCl}_3$  at  $20^\circ\text{C}$  in the mode of internal stabilization at the  $^2\text{H}$  resonance line; the chemical shifts  $\delta$  and spin-spin coupling constants were measured with an accuracy of 0.01 ppm and 0.1 Hz, respectively.

The electronic absorption spectra were measured on Specord M40, Varian Carry 100, and Hewlett—Packard 8452A spectrophotometers. The solvents MeOH, EtOH, MeCN,  $\text{Me}_2\text{CO}$ , PhMe, and heptane were purchased from Aldrich. Photolysis of solutions and polymeric films was carried out using a DRSh-250



mercury lamp equipped with light filters to separate lines of the mercury spectrum. The kinetics of photocoloration and dark decoloration of SPO in polymeric films was recorded on an apparatus constructed based on a Hitachi Perkin–Elmer 139 spectrophotometer.<sup>24</sup>

Poly(methyl methacrylate) was used as the polymeric matrix. The films were prepared by slow evaporation of  $\text{CHCl}_3$  from solutions of the polymer and SPO followed by drying of the samples. The concentration of the compounds in the polymeric matrix was  $(1\text{--}5) \cdot 10^{-3} \text{ mol L}^{-1}$ .

The efficiency of photocoloration of SPO **9–15** was estimated using the parameter  $\eta$ , which was calculated as the ratio between the photocolorability of the compound under study ( $H^X$ ) and the photocolorability of the reference compound ( $H^E$ ), 6-nitroBIPS being used as the standard. The photocolorability, which is the product of the quantum yield of formation of colored product **B** ( $\Phi_{A \rightarrow B}$ ) by the molar extinction coefficient ( $\epsilon_{\text{max}}$ ) at the long-wavelength absorption maximum of form **B**,<sup>2a</sup> was determined according to the equation<sup>1</sup>

$$\eta = H^X/H^E = (\Phi_{A \rightarrow B}^X \cdot \epsilon_{\text{max}}^X) / (\Phi_{A \rightarrow B}^E \cdot \epsilon_{\text{max}}^E).$$

Samples were subjected to photolysis at  $\lambda = 365 \text{ nm}$ . The intensity of incident light measured on an Aberchrome 540 actinometer was  $6 \cdot 10^{15} \text{ quantum s}^{-1}$ .

The lifetime of the colored form in polymeric films was estimated using the parameter  $\tau_{1/2}^B$ , viz., the time during which the absorbance at the absorption maximum of colored form **B** was halved.

**Synthesis of compounds 9–15 (general procedure).** A mixture of the corresponding 3*H*-indolium iodide **1–7** (1 mmol),  $\text{Et}_3\text{N}$  (1.5 mmol), 1-amino-4-cyano-2-naphthol hydrochloride (**8**) (1.1 mmol),  $\text{CaSO}_4$  (0.3 g),  $\text{NaHCO}_3$  (0.4 g), and DMSO (0.23 mL) in PhMe (10 mL) was heated at  $80^\circ\text{C}$  for 12 h under an inert atmosphere (chromatographic control). The solution was filtered and concentrated *in vacuo*. The residue was purified by column chromatography on  $\text{Al}_2\text{O}_3$  (hexane–acetone as the eluent, 10 : 1).

**6'-Cyano-5-methoxy-3,3-dimethyl-1-propylspiro[indoline-2,3'-[3*H*]naphtho[2,1-*b*][1,4]oxazine] (9).** The yield was 47%, m.p.  $126\text{--}127^\circ\text{C}$  (from heptane). Found (%): C, 75.96; H, 6.07; N, 10.30.  $\text{C}_{26}\text{H}_{25}\text{N}_3\text{O}_2$ . Calculated (%): C, 75.89; H, 6.12; N, 10.21.  $^1\text{H}$  NMR,  $\delta$ : 0.89 (t, 3 H, Pr,  $J = 7.4 \text{ Hz}$ ); 1.28 and 1.35 (both s, 3 H each, Me); 1.65 (m, 2 H, Pr); 3.07 (t, 2 H, Pr,  $J = 7.4 \text{ Hz}$ ); 3.78 (s, 3 H, OMe); 6.50 (d, 1 H, H(7'),  $J = 8.2 \text{ Hz}$ ); 6.69–6.74 (m, 2 H, H(4), H(6)); 7.42 (s, 1 H, H(5')); 7.57 and 7.67 (both dt, 1 H each, H(8'), H(9'),  $J = 6.9 \text{ Hz}$ ,  $J = 1.3 \text{ Hz}$ ); 7.86 (s, 1 H, H(2')); 8.12 and 8.64 (both d, 1 H each, H(7'), H(10'),  $J = 8.2 \text{ Hz}$ ).

**6'-Cyano-1-isobutyl-5-methoxy-3,3-dimethylspiro[indoline-2,3'-[3*H*]naphtho[2,1-*b*][1,4]oxazine] (10).** The yield was 46%, m.p.  $184\text{--}185^\circ\text{C}$  (from heptane). Found (%): C, 76.32; H, 6.26; N, 9.97.  $\text{C}_{27}\text{H}_{27}\text{N}_3\text{O}_2$ . Calculated (%): C, 76.21; H, 6.40; N, 9.87.  $^1\text{H}$  NMR,  $\delta$ : 0.89 and 0.95 (both d, 3 H each,  $\text{Bu}^i$ ,  $J = 6.9 \text{ Hz}$ ); 1.28 and 1.37 (both s, 3 H each, Me); 2.02 (m, 1 H,  $\text{Bu}^i$ ); 2.69 (dd, 1 H,  $\text{Bu}^i$ ,  $J = 14.3 \text{ Hz}$ ,  $J = 9.5 \text{ Hz}$ ); 2.95 (dd, 1 H,  $\text{Bu}^i$ ,  $J = 14.3 \text{ Hz}$ ,  $J = 5.6 \text{ Hz}$ ); 3.78 (s, 3 H, OMe); 6.49 (d, 1 H, H(7'),  $J = 8.6 \text{ Hz}$ ); 6.68–6.72 (m, 2 H, H(4), H(6)); 7.42 (s, 1 H, H(5')); 7.57 and 7.67 (both dt, 1 H each, H(8'), H(9'),  $J = 6.9 \text{ Hz}$ ,  $J = 1.3 \text{ Hz}$ ); 8.11 (s, 1 H, H(2')); 8.12 and 8.64 (both d, 1 H each, H(7'), H(10'),  $J = 8.2 \text{ Hz}$ ).

**6'-Cyano-1,3,3-trimethyl-5-propoxyspiro[indoline-2,3'-[3*H*]naphtho[2,1-*b*][1,4]oxazine] (11).** The yield was 46%, m.p.  $160\text{--}161^\circ\text{C}$  (from heptane). Found (%): C, 75.77; H, 6.19; N, 10.14.  $\text{C}_{26}\text{H}_{25}\text{N}_3\text{O}_2$ . Calculated (%): C, 75.89; H, 6.12; N, 10.21.  $^1\text{H}$  NMR,  $\delta$ : 1.03 (t, 3 H, OPr,  $J = 7.4 \text{ Hz}$ ); 1.30 and 1.35 (both s, 3 H each, Me); 1.79 (m, 2 H, OPr); 2.67 (s, 3 H, NMe); 3.88 (t, 2 H, OPr,  $J = 6.6 \text{ Hz}$ ); 6.47 (d, 1 H, H(7'),  $J = 8.1 \text{ Hz}$ ); 6.71–6.75 (m, 2 H, H(4), H(6)); 7.45 (s, 1 H, H(5')); 7.58 and 7.67 (both dt, 1 H each, H(8'), H(9'),  $J = 6.9 \text{ Hz}$ ,  $J = 1.3 \text{ Hz}$ ); 7.86 (s, 1 H, H(2')); 8.12 and 8.64 (both d, 1 H each, H(7'), H(10'),  $J = 8.2 \text{ Hz}$ ).

**6'-Cyano-1,3,3-trimethyl-5-nonyloxyspiro[indoline-2,3'-[3*H*]naphtho[2,1-*b*][1,4]oxazine] (12).** The yield was 43%, m.p.  $135\text{--}136^\circ\text{C}$  (from propan-2-ol). Found (%): C, 77.66; H, 7.38; N, 8.56.  $\text{C}_{32}\text{H}_{37}\text{N}_3\text{O}_2$ . Calculated (%): C, 77.54; H, 7.52; N, 8.48.  $^1\text{H}$  NMR,  $\delta$ : 0.87 (t, 3 H,  $\text{OC}_9\text{H}_{19}$ ,  $J = 6.9 \text{ Hz}$ ); 1.25–1.28 (m, 10 H,  $\text{OC}_9\text{H}_{19}$ ); 1.30 and 1.35 (both s, 3 H each, Me); 1.45 and 1.76 (both m, 2 H each,  $\text{OC}_9\text{H}_{19}$ ); 2.67 (s, 3 H, NMe); 3.91 (t, 2 H,  $\text{OC}_9\text{H}_{19}$ ,  $J = 6.6 \text{ Hz}$ ); 6.46 (d, 1 H, H(7'),  $J = 8.1 \text{ Hz}$ ); 6.70–6.75 (m, 2 H, H(4), H(6)); 7.44 (s, 1 H, H(5')); 7.57 and 7.67 (both dt, 1 H each, H(8'), H(9'),  $J = 6.9 \text{ Hz}$ ,  $J = 1.3 \text{ Hz}$ ); 7.85 (s, 1 H, H(2')); 8.12 and 8.64 (both d, 1 H each, H(7'), H(10'),  $J = 8.2 \text{ Hz}$ ).

**6'-Cyano-5-hexadecyloxy-1,3,3-trimethylspiro[indoline-2,3'-[3*H*]naphtho[2,1-*b*][1,4]oxazine] (13).** The yield was 45%, m.p.  $85\text{--}86^\circ\text{C}$  (from propan-2-ol). Found (%): C, 78.93; H, 8.57; N, 7.15.  $\text{C}_{39}\text{H}_{51}\text{N}_3\text{O}_2$ . Calculated (%): C, 78.88; H, 8.66; N, 7.08.  $^1\text{H}$  NMR,  $\delta$ : 0.86 (t, 3 H,  $\text{OC}_{16}\text{H}_{33}$ ,  $J = 6.9 \text{ Hz}$ ); 1.22–1.28 (m, 24 H,  $\text{OC}_{16}\text{H}_{33}$ ); 1.30 and 1.35 (both s, 3 H each, Me); 1.44 and 1.76 (both m, 2 H each,  $\text{OC}_{16}\text{H}_{33}$ ); 2.67 (s, 3 H, NMe); 3.91 (t, 2 H,  $\text{OC}_{16}\text{H}_{33}$ ,  $J = 6.6 \text{ Hz}$ ); 6.46 (d, 1 H, H(7'),  $J = 8.1 \text{ Hz}$ ); 6.70–6.75 (m, 2 H, H(4), H(6)); 7.45 (s, 1 H, H(5')); 7.58 and 7.67 (both dt, 1 H each, H(8'), H(9'),  $J = 6.9 \text{ Hz}$ ,  $J = 1.3 \text{ Hz}$ ); 7.86 (s, 1 H, H(2')); 8.12 and 8.64 (both d, 1 H each, H(7'), H(10'),  $J = 8.1 \text{ Hz}$ ).

**6'-Cyano-1,3,3,5,4(6)-pentamethylspiro[indoline-2,3'-[3*H*]naphtho[2,1-*b*][1,4]oxazines] (14a,b).**\* The yield was 37%, m.p.  $176\text{--}179^\circ\text{C}$  (from heptane). Found (%): C, 78.82; H, 6.00; N, 11.13.  $\text{C}_{25}\text{H}_{23}\text{N}_3\text{O}$ . Calculated (%): C, 78.71; H, 6.08; N, 11.02.  $^1\text{H}$  NMR,  $\delta$ : 1.30 and 1.34 (both s, 3 H each, 3-Me (**14b**)); 1.42 and 1.45 (both s, 3 H each, 3-Me (**14a**)); 2.22, 2.23, 2.25, and 2.26 (all s, 3 H each, 6-Me (**14b**), 4-Me (**14a**), 5-Me (**14a,b**)); 2.66 and 2.70 (both s, 3 H each, NMe (**14a,b**)); 6.35 (d, 1 H, H(7') (**14a**),  $J = 7.8 \text{ Hz}$ ); 6.40 (s, 1 H, H(7') (**14b**)); 6.85 (s, 1 H, H(4') (**14b**)); 7.02 (d, 1 H, H(6') (**14a**),  $J = 7.8 \text{ Hz}$ ); 7.43 and 7.44 (both s, 1 H each, H(5') (**14a,b**)); 7.57 and 7.67 (both m, 1 H each, H(8'), H(9') (**14a,b**)); 7.86 (s, 1 H, H(2') (**14a,b**)); 8.12 (d, 1 H, H(7') (**14a,b**),  $J = 8.2 \text{ Hz}$ ); 8.64 (d, 1 H, H(10') (**14a,b**),  $J = 8.5 \text{ Hz}$ ).

**6'-Cyano-4(6)-methoxy-1,3,3-trimethylspiro[indoline-2,3'-[3*H*]naphtho[2,1-*b*][1,4]oxazines] (15a,b).**\* The yield was 24%, m.p.  $146\text{--}149^\circ\text{C}$  (from heptane). Found (%): C, 75.32; H, 5.39; N, 11.04.  $\text{C}_{24}\text{H}_{21}\text{N}_3\text{O}_2$ . Calculated (%): C, 75.18; H, 5.52; N, 10.96.  $^1\text{H}$  NMR,  $\delta$ : 1.29 and 1.33 (both s, 3 H each, 3-Me (**15b**)); 1.39 and 1.42 (both s, 3 H each, 3-Me (**15a**)); 2.71 and 2.72 (both s, 3 H each, NMe (**15a,b**)); 3.80 and 3.81 (both s, 3 H each, 6-OMe (**15b**), 4-OMe (**15a**)); 6.16 (d, 1 H, H(7') (**15b**),  $J = 2.2 \text{ Hz}$ ); 6.24 (d, 1 H, H(7') (**15a**),  $J = 8.3 \text{ Hz}$ ); 6.41 (dd, 1 H, H(5') (**15b**),  $J = 8.1 \text{ Hz}$ ,  $J = 2.2 \text{ Hz}$ ); 6.47 (d, 1 H,

\* A mixture of isomers.

H(5) (**15a**),  $J = 8.3$  Hz); 6.95 (d, 1 H, H(4) (**15b**),  $J = 8.1$  Hz); 7.17 (t, 1 H, H(6) (**15a**),  $J = 8.1$  Hz); 7.45 and 7.46 (both s, 1 H each, H(5') (**15a,b**)); 7.57 and 7.58 (both dt, 1 H each, H(8') (**15a,b**),  $J = 6.9$  Hz,  $J = 1.3$  Hz); 7.66 (dt, 1 H, H(9') (**15a,b**),  $J = 6.9$  Hz,  $J = 1.3$  Hz); 7.83 (s, 1 H, H(2') (**15a,b**)); 8.12 and 8.64 (both d, 1 H each, H(7'), H(10') (**15a,b**),  $J = 8.1$  Hz).

**X-ray diffraction study of compound 10.** The data from X-ray diffraction study are given in Tables 1–3. Crystals of spirooxazine **10** were grown by crystallization from heptane. The X-ray data were collected on an automated four-circle KUMA diffractometer (Mo-K $\alpha$  radiation) at  $T = 293$  K in the angle range  $1.81^\circ \leq \theta \leq 27.03^\circ$ . The structure of **10** was solved by direct methods and refined by the least-squares method to  $R = 0.042$  based on 4270 reflections ( $R_w = 0.0896$  based on 4430 reflections,  $\text{GOF}(F^2) = 0.877$ ) with anisotropic thermal parameters for nonhydrogen atoms using the SHELXL93 program package.<sup>25</sup> The H atoms were revealed from the difference Fourier synthesis and only their positional parameters were refined.

This study was financially supported by INTAS (Grant 00-00152) and the Russian Foundation for Basic Research (Project No. 03-03-32154).

## References

1. N. A. Voloshin, A. V. Metelitsa, J. C. Micheau, E. N. Voloshina, S. O. Besugliy, A. V. Vdovenko, N. E. Shelepin, and V. I. Minkin, *Izv. Akad. Nauk, Ser. Khim.*, 2003, 1110 [*Russ. Chem. Bull., Int. Ed.*, 2003, **52**, 1172].
2. *Photochromism: Molecules and Systems*, Eds. H. Dürr and H. Bouas-Laurent, Elsevier, Amsterdam, 1990, (a) Ch. 8; (b) Ch. 10.
3. *Organic Photochromic and Thermochromic Compounds. Vol. 1: Main Photochromic Compounds*, Eds. J. C. Crano and R. J. Guglielmetti, Plenum Press, New York, 1999, 378 pp.; (a) 105.
4. *Organic Photochromic and Thermochromic Compounds. Vol. 2: Physicochemical Studies, Biological Applications, and Thermochromism*, Eds. J. C. Crano and R. J. Guglielmetti, Kluwer Academic, New York, 1999, 473 pp.; (a) Ch. 7.
5. G. Berkovic, V. Krongauz, and V. Weiss, *Chem. Rev.*, 2000, **100**, 1741.
6. S. Kawata and Y. Kawata, *Chem. Rev.*, 2000, **100**, 1777.
7. V. Lokshin, A. Samat, and A. V. Metelitsa, *Usp. Khim.*, 2002, **71**, 1015 [*Russ. Chem. Rev.*, 2002, **71** (Engl. Transl.)].
8. H. Yajima, N. Yoshimoto, and T. Ishii, *J. Photopolym. Sci. Technol.*, 1998, **11**, 47.
9. A. V. Metelitsa, J. C. Micheau, N. A. Voloshin, E. N. Voloshina, and V. I. Minkin, *J. Phys. Chem. A.*, 2001, **105**, 8417.
10. G. Favaro, F. Masetti, V. Mazzucato, G. Ottavi, P. Aliegrini, and V. Malatesta, *J. Chem. Soc., Faraday Trans.*, 1994, **90**, 333.
11. V. Lokshin, A. Samat, and R. Guglielmetti, *Tetrahedron*, 1997, **53**, 9669.
12. PTI Int. Appl. WO 96/04590; *Chem. Abstrs.*, 1996, **124**, 356317.
13. PTI Int. Appl. WO 96/03368; *Chem. Abstrs.*, 1996, **125**, 33661.
14. D. Shragina, F. Buchgoltz, S. Yitzchaik, and V. Krongauz, *Liq. Cryst.*, 1990, **7**, 643.
15. W. Bradley and R. Robinson, *J. Chem. Soc.*, 1934, 1484.
16. E. Pottier, M. Sergeant, R. Phan Tan Luu, and R. Guglielmetti, *Bull. Soc. Chim. Belg.*, 1992, **101**, 719.
17. S. M. Aldoshin, I. I. Chuev, O. S. Filipenko, A. N. Utenyshev, V. Lokshin, P. Laregenie, A. Samat, and R. Guglielmetti, *Izv. Akad. Nauk, Ser. Khim.*, 1998, 1121 [*Russ. Chem. Bull.*, 1998, **47**, 1089 (Engl. Transl.)].
18. F. H. Allen, O. Kennard, D. Watson, L. Brammer, G. Orpen, and R. Taylor, *J. Chem. Soc., Perkin Trans. 2*, 1987, 1.
19. N. Y. C. Chu, *Can. J. Chem.*, 1983, **61**, 300.
20. L. G. S. Brooker, A. C. Craig, D. W. Heseltine, P. W. Jenkins, and L. L. Lincoln, *J. Am. Chem. Soc.*, 1965, **87**, 2443.
21. G. Smets, *Adv. Polym. Sci.*, 1983, **50**, 17.
22. G. Williams and D. C. Watts, *Trans. Faraday Soc.*, 1970, **66**, 80.
23. Y. Munakata, T. Tsutsui, and S. Saito, *Polymer J.*, 1990, **22**, 843.
24. A. V. Metelitsa, N. A. Voloshin, N. E. Shelepin, M. I. Knyazhanskii, and V. I. Minkin, *Khim. Geterotsikl. Soedin.*, 1996, 399 [*Chem. Heterocycl. Compd.*, 1996, **32** (Engl. Transl.)].
25. G. M. Sheldrick, *SHELXL93. Program for the Refinement of Crystal Structures*, Göttingen University, Göttingen (Germany), 1993.

Received October 14, 2002;  
in revised form May 19, 2003